

Production of the D_s^\pm by High Energy Neutrons*

C. Shipbaugh⁽²⁾, J. Wiss⁽²⁾, M. Binkley⁽³⁾, J. Butler⁽³⁾,
J. P. Cumalat⁽¹⁾, P. Coteus⁽¹⁾, M. DiCorato^{(5),(6)},
M. Diesburg⁽²⁾, J. Enagonio^{(1),(3)}, J. Filaseta^{(2),(a)},
P. L. Frabetti⁽⁴⁾, I. Gaines⁽³⁾, P. Garbincius⁽³⁾, M. Gormley⁽³⁾,
D. J. Harding⁽³⁾, T. Kroc⁽²⁾, R. Ladbury⁽¹⁾, P. Lebrun⁽³⁾,
P. F. Manfredi^{(5),(6)}, J. Peoples⁽³⁾, A. Sala⁽⁶⁾, J. Slaughter^{(3),(b)}

⁽¹⁾University of Colorado
Boulder, Colorado 80303

⁽²⁾University of Illinois at Urbana-Champaign
Urbana, Illinois 61801

⁽³⁾Fermi National Accelerator Laboratory
Batavia, Illinois 60510

⁽⁴⁾Universita di Bologna, Dipartimento di Fisica and I.N.F.N.
Bologna, Italy

⁽⁵⁾Universita di Milano, Dipartimento di Fisica
Milano, Italy

⁽⁶⁾Istituto Nazionale di Fisica Nucleare
Milano, Italy

December 1987

*Submitted to Phys. Rev. Lett.



Production of the D_s^\pm by High Energy Neutrons

C. SHIPBAUGH⁽²⁾, J. WISS⁽²⁾, M. BINKLEY⁽³⁾, J. BUTLER⁽³⁾,
J. P. CUMALAT⁽¹⁾, P. COTEUS⁽¹⁾, M. DICORATO^{(5),(6)},
M. DIESBURG⁽²⁾, J. ENAGONIO^{(1),(3)}, J. FILASETA^{(2),(a)},
P. L. FRABETTI⁽⁴⁾, I. GAINES⁽³⁾, P. GARBINCIUS⁽³⁾, M. GORMLEY⁽³⁾,
D. HARDING⁽³⁾, T. KROC⁽²⁾, R. LADBURY⁽¹⁾, P. LEBRUN⁽³⁾,
P. F. MANFREDI^{(5),(6)}, J. PEOPLES⁽³⁾, A. SALA⁽⁶⁾, J. SLAUGHTER^{(3),(b)}

⁽¹⁾ *University of Colorado, Boulder, Colorado 80303*

⁽²⁾ *University of Illinois at Urbana-Champaign, Urbana, Illinois 61801*

⁽³⁾ *Fermilab, Batavia, Illinois 60510*

⁽⁴⁾ *Universita di Bologna, Dipartimento di Fisica and I.N.F.N., Bologna, Italy*

⁽⁵⁾ *Universita di Milano, Dipartimento di Fisica, Milano, Italy*

⁽⁶⁾ *Istituto Nazionale di Fisica Nucleare, Milano, Italy*

ABSTRACT

We have observed the production of the D_s^\pm by a high energy neutron beam on nuclear targets. The D_s^\pm was observed in the decay mode $D_s^\pm \rightarrow \phi\pi^\pm$, $\phi \rightarrow K^+K^-$. The average of the inclusive cross sections for D_s^+ and D_s^- hadroproduction is measured to be $B \cdot \frac{d\sigma}{dx_f} = 2.85 \pm .80 \pm .86 \mu\text{b/nucleon}$ at $x_f = .175$ assuming a linear A dependence, where $B \equiv \Gamma(D_s^\pm \rightarrow \phi\pi^\pm)/\Gamma(D_s^\pm \rightarrow \text{all})$.

PACS numbers: 13.30.Eg, 14.40.Jz

Submitted to *Physical Review Letters*

We have measured the cross section times branching fraction for hadroproduction of the decay mode $D_s^\pm \rightarrow \phi\pi^\pm$. This mode has been previously observed¹ in e^+e^- annihilation to have a mass of $1970 \pm 5 \text{ MeV}/c^2 \pm 5 \text{ MeV}/c^2$ and has since been confirmed by several observations. Several experiments have measured the branching fraction for $D_s^\pm \rightarrow \phi\pi^\pm$, but the value is not yet well-determined.^{1,2,3,4} Previously published information on the hadroproduction of the D_s^+ has been severely statistics limited.^{5,6} We have observed a 64 event $D_s^\pm \rightarrow \phi\pi^\pm$ signal at a mass of $1972 \text{ MeV}/c^2 \pm 5 \text{ MeV}/c^2$ produced by high energy neutrons.

The experiment E400 was performed in the Proton East beamline at Fermi National Accelerator Laboratory. The incident neutron beam was formed by 800 GeV protons incident on a beryllium target. The neutron energy spectrum ranged from 0 to 800 GeV and was triangular in shape, with a most probable energy at 640 GeV (\sqrt{s} of 35 GeV). The contribution to the neutral beam from photons and K_L^0 's above 200 GeV was negligible.

A layout of the apparatus and detailed description of the spectrometer have been given previously⁷. Briefly, the detector consists of an active target and vertex detector, a magnetic spectrometer, a gas Cerenkov system, and electromagnetic and hadronic calorimetry. The target was composed of three segments consisting of tungsten, silicon, and beryllium. The total event energy was obtained by summing the output of the electromagnetic, hadronic, and beam dump calorimetry. The summed response of the electromagnetic and hadronic calorimeters was used as our minimum energy trigger.

Charged particle identification was accomplished using three 34 cell Cerenkov counters, operating (from upstream to downstream) with pion thresholds of 2.8,

10.8, and 5.7 GeV/c respectively. Protons could be uniquely identified from 10 to 80 GeV/c, while unique kaon identification extended from 10 to 40 GeV/c.

The data for this analysis consisted of approximately 45 million events. The event trigger required that all of the following conditions be satisfied: (a) a coincidence between a target region scintillation counter and two coincidences in a downstream scintillator hodoscope; (b) a minimum calorimeter trigger energy of 265 GeV; (c) a minimum multiplicity of four charged tracks in the downstream spectrometer; (d) a deposited charge in the most downstream active silicon target equivalent to 2 or more charged tracks; (e) at least one charged kaon with momentum over 21 GeV/c or one proton over 40 GeV/c traversing the entire detector. All triggers satisfying requirements a) through e) were subject to a procedure which found all charged tracks and a common vertex, and which then performed a Cerenkov counter analysis.

Figure 1 shows a K^+K^- invariant mass distribution with a prominent ϕ signal. Each kaon candidate is required to be uniquely Cerenkov identified (i.e., unambiguous with either the pion or proton hypothesis). Because this state has a natural width comparable to our spectrometer resolution, we have performed the fit to the signal by the convolution of a Breit-Wigner shape of appropriate width⁸ with a Gaussian distribution. The background has been fit by a third-order polynomial. The result is 33,000 candidates with a mass at 1019.5 MeV/c². We selected ϕ candidates by applying a K^+K^- mass cut of 1019.5 ± 3.5 MeV/c².

To perform the D_s^\pm search, these ϕ candidates were combined with charged tracks, assuming a pion mass. Those tracks positively identified as either a kaon or proton using information from the Cerenkov counters were excluded. The

resulting $\phi\pi^\pm$ invariant mass histogram is shown in Figure 2. A multiplicity requirement of less than 14 tracks has been applied to reduce the combinatoric background. This distribution has been fit with a Gaussian peak representing $D_s^\pm \rightarrow \phi\pi^\pm$ decay over a smooth background. We have included an additional peak located near the known D^+ mass in order to represent the $D^\pm \rightarrow \phi\pi^\pm$ process. The width of the D_s^\pm and D^\pm peaks were constrained to be identical. The fit gives 65 ± 29 D_s^\pm candidates with a mass of 1981 ± 3 MeV/ c^2 and a width of 8.5 ± 2.7 MeV/ c^2 , and also 69 ± 38 D^\pm candidates with a mass of 1973 ± 8 MeV/ c^2 .

For the decay $D_s^+ \rightarrow \phi\pi^+$, the angle θ between the K^+ and the π^+ , when viewed in the ϕ rest frame, is expected to follow the distribution given by $\frac{dN}{d\cos\theta} \propto \cos^2\theta$. The rather significant forward-backward peaking present in the $\cos\theta$ distribution can be exploited to improve the signal to background ratio in the D_s^\pm search, because our spectrometer has flat acceptance in θ .

Figure 3 is a fit to the $\phi\pi^\pm$ invariant mass histogram requiring that $|\cos\theta| \geq .5$. We observe 64 ± 16 D_s^\pm events for a significance of 4.0 standard deviations. The mass is 1972 ± 5 MeV/ c^2 and the width is 8.4 ± 3.5 MeV/ c^2 , which is consistent with our detector resolution for this state. The fit also gives 47 ± 23 D^\pm events at the mass 1876 ± 4 MeV/ c^2 . Comparison of the data of Figure 2 and Figure 3, shows that $(98 \pm 37)\%$ of the D_s^\pm signal and only 50 % of the background survives the $\cos\theta$ cut. The survival fraction obtained in the data for the signal is consistent with the expected value of 87.5 % obtained by integrating the $D_s^\pm \rightarrow \phi\pi^\pm$ angular decay distribution.

Although the significance of the $D^\pm \rightarrow \phi\pi^\pm$ signal present in Figure 3 is only ≈ 2 standard deviations, it may be of interest to compare the yield of D_s^\pm

and D^\pm events. Correcting the raw number of signal events obtained from the fit of Figure 3 for possible differences in D_s^\pm and D^\pm acceptance and triggering efficiencies using the weighting method described later in this paper, we obtain an acceptance corrected event fraction of $N_{D^\pm}/(N_{D^\pm} + N_{D_s^\pm}) = .38 \pm .17$, where both N_{D^\pm} and $N_{D_s^\pm}$ refer to the number of decays observed in the $\phi\pi^\pm$ decay mode over the x_f range from 0.05 to 0.30.

We have obtained an estimate for $B \cdot \sigma$ for the $D_s^\pm \rightarrow \phi\pi^\pm$ process in the region $0.05 < x_f < 0.30$ by dividing the acceptance corrected event yield by the luminosity determined by counting relatively unbiased inelastic neutron interactions originating in our target. The x_f for a given combination was computed from the measured energy of a D_s^\pm candidate, and the incident neutron energy as reconstructed through calorimetry. Here $B \equiv \Gamma(D_s^\pm \rightarrow \phi\pi^\pm)/\Gamma(D_s^\pm \rightarrow \text{all})$, and our cross sections are presented with the value .495 for the branching fraction $\Gamma(\phi \rightarrow K^+K^-)/\Gamma(\phi \rightarrow \text{all})$ incorporated. A relatively model independent measurement of the corrected event yield was made by fitting a weighted $\phi\pi^\pm$ invariant mass distribution for all combinations which satisfy the particle identification, angular distribution, and multiplicity cuts. The combinations entering this histogram were individually weighted by the reciprocal of the D_s^\pm acceptance, which was parameterized as a function of $x_f(D_s^\pm)$ alone, and in this way averaged over all other relevant production and decay variables. As a check, we obtained an alternative acceptance corrected event yield by fitting a weighted $\phi\pi^\pm$ mass distribution for D_s^\pm candidates with weights parameterized in terms of the measured the D_s^\pm energy rather than x_f . We required events to have a D_s^\pm energy between 45 and 145 GeV – an energy range chosen to correspond to the previous x_f range at our average neutron energy. This alternative yield estimate

was found to be completely consistent but 15 % lower than the yield estimate from the x_f parameterized acceptance correction technique.

The sample luminosity was measured by counting the number of unbiased neutron interactions as recorded by the coincidence between the target region scintillation counter and downstream scintillation hodoscope and dividing by the previously measured⁹ total inelastic neutron cross sections averaged over our target materials after correction for triggering losses (0.15) and livetime (0.40). We obtain a partial cross section of $B \cdot (\sigma(D_s^+) + \sigma(D_s^-)) = 1.51 \pm .43 \mu\text{b/nucleon}$ in the range $0.05 < x_f < 0.30$, where we have assumed a linear A dependence for the hadronic charm cross section. Within the kinematic region covered by our data we find the ratio of charges to be $D_s^+/D_s^- = 1.9 \pm 1.5$, which is consistent with symmetric particle and antiparticle production. Under this symmetric production assumption, the D_s^+ inclusive production cross section would be $B \cdot \frac{1}{2}(\sigma(D_s^+) + \sigma(D_s^-)) = .76 \pm .21 \mu\text{b/nucleon}$. Correcting for the x_f range, we obtain the differential cross section :

$$B \cdot \frac{1}{2} \left(\frac{d\sigma(D_s^+)}{dx_f} + \frac{d\sigma(D_s^-)}{dx_f} \right) = 2.85 \pm 0.80 \pm .86 \mu\text{b/nucleon at } x_f = 0.175$$

In addition to the statistical error ($\pm .80$) we have included a systematic uncertainty in the cross section of $\approx 30\%$ due to errors in the luminosity ($\pm 20\%$), model dependence ($\pm 20\%$), and differences due to the parameterization of the acceptance ($\pm 10\%$). This value assumes a nuclear dependence of the form $A^{1.0}$. The cross section is sensitive to the value of α assumed for the nuclear A^α dependence. A $\pm 10\%$ change of α about 1.0 will result in a $\pm 30\%$ change in σ .

It is interesting to compare this value for the hadronic D_s^+ production cross section to the hadronic cross section for other charmed species. We have previ-

ously measured¹⁰ the average of the D^{*+} and D^{*-} inclusive cross sections to be $B \cdot \frac{d\sigma}{dx_f} = 2.11 \pm .43 \pm .63 \mu\text{b/nucleon}$ at $x_f = 0.07$ in the decay sequence $D^{*+} \rightarrow D^0\pi^+$, $D^0 \rightarrow K^+K^-$. Extrapolating both the D_s^\pm and $D^{*\pm}$ differential cross sections to $x_f = 0$ by assuming a common x_f dependence of the form $d\sigma/dx_f \propto (1 - |x_f|)^N$ with N in the range from 3 to 5, we obtain the ratio:

$$\frac{B(D_s) \cdot \frac{d\sigma}{dx_f}(D_s)}{B(D^*) \cdot \frac{d\sigma}{dx_f}(D^*)} = 2.18 \pm 1.08 \text{ at } x_f = 0.$$

After correcting by the measured D^* branching ratio⁸, $B(D^*) = 0.314\%$, and a composite of estimates¹¹ for the D_s , $B(D_s) = 3.6\%$, we obtain the ratio:

$$\frac{\frac{d\sigma}{dx_f}(D_s)}{\frac{d\sigma}{dx_f}(D^*)} = 0.19 \pm 0.09 \text{ at } x_f = 0.$$

We have not included errors on the relevant charm branching ratios since we know of no way of estimating these errors for the $D_s \rightarrow \phi\pi$ decay mode.

In conclusion, we have measured the average of the D_s^+ and D_s^- hadroproduced inclusive cross sections into the mode $D_s^\pm \rightarrow \phi\pi^\pm$ to be

$$B \cdot \frac{d\sigma}{dx_f} = 2.85 \pm 0.80 \pm .86 \mu\text{b/nucleon at } x_f = 0.175$$

for high energy neutrons incident on a fixed target assuming a linear A dependence.

We gratefully acknowledge the assistance we received from the Fermilab staff and the support staffs at the University of Illinois, at the University of Colorado, and at INFN in Milan. This research is supported by the U.S. Department of Energy and by the Istituto Nazionale di Fisica Nucleare of Italy. One of us (J. W.) wishes to acknowledge support from the A. P. Sloan Foundation from 1982-1986.

a) Present address: Northern Kentucky University, Highland Heights, KY
41076

b) Permanent address: Yale University, New Haven, CT 06511

REFERENCES

1. A. Chen *et al.*, Phys. Rev. Lett. **51**, 634 (1983)
2. M. Althoff *et al.*, Phys. Lett. **136B**, 130 (1984)
3. M. Derrick *et al.*, Phys. Rev. Lett. **54**, 2568 (1985)
4. H. Albrecht *et al.*, Phys. Lett. **153B**, 343 (1985)
5. R. Bailey *et al.*, Phys. Lett. **139B**, 320 (1984)
6. M. Aguilar-Benitez *et al.*, Phys. Lett. **156B**, 444 (1985)
7. P. Coteus *et al.*, Phys. Rev. Lett. **59**, 1530 (1987)
8. PDG, Phys. Lett. **170B** (1986)
9. R. Ammar *et al.*, Phys. Lett. **178B** (1986) 124
10. J. Cumalat *et al.*, submitted to Phys. Rev. Lett.
11. PDG, Phys. Lett. **170B**, 147 (1986)

FIGURE CAPTIONS

1. K^+K^- mass spectrum.
2. $\phi\pi^\pm$ mass spectrum.
3. $\phi\pi^\pm$ mass spectrum with ϕ decay angle cut.

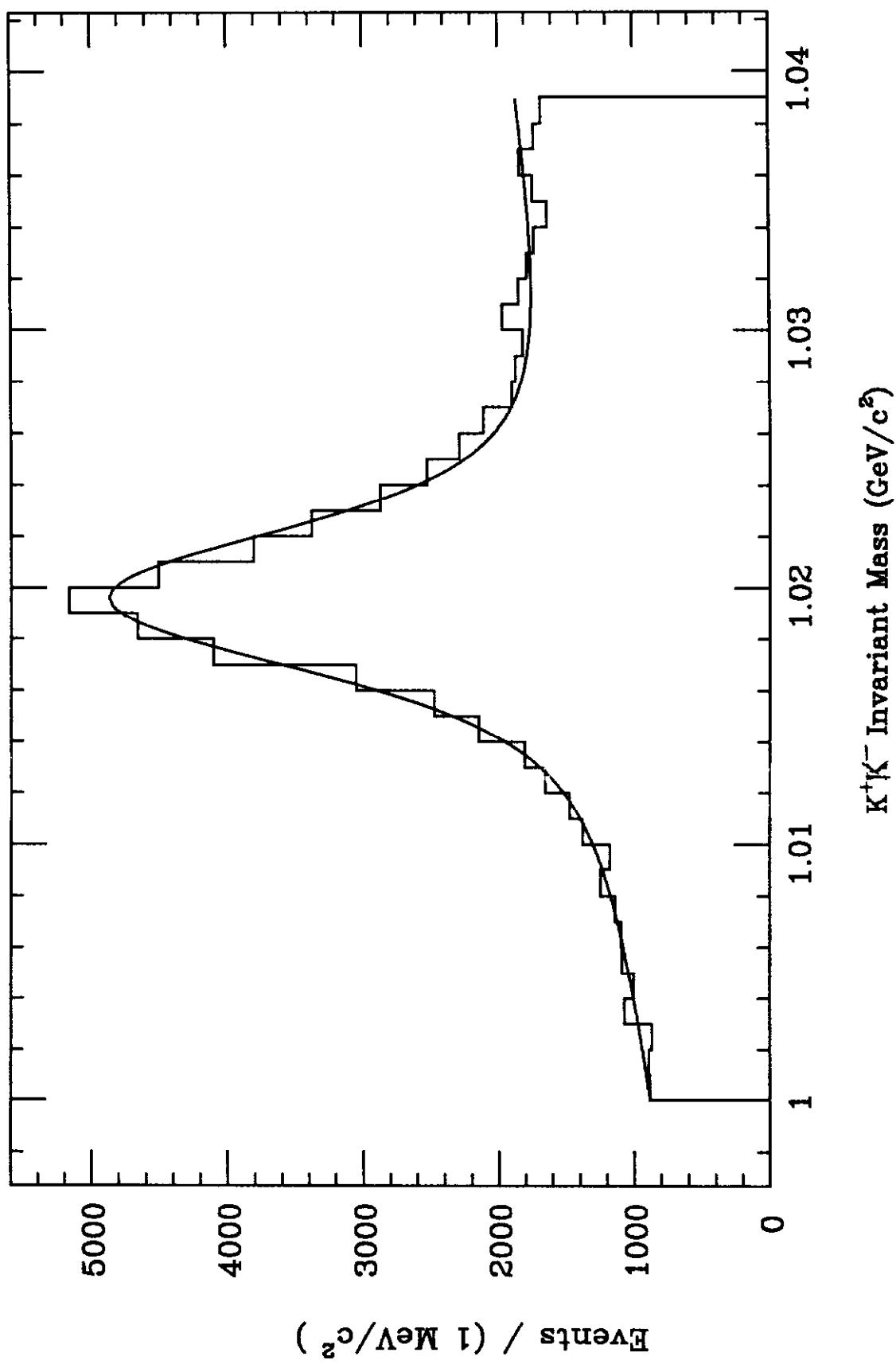


Fig. 1

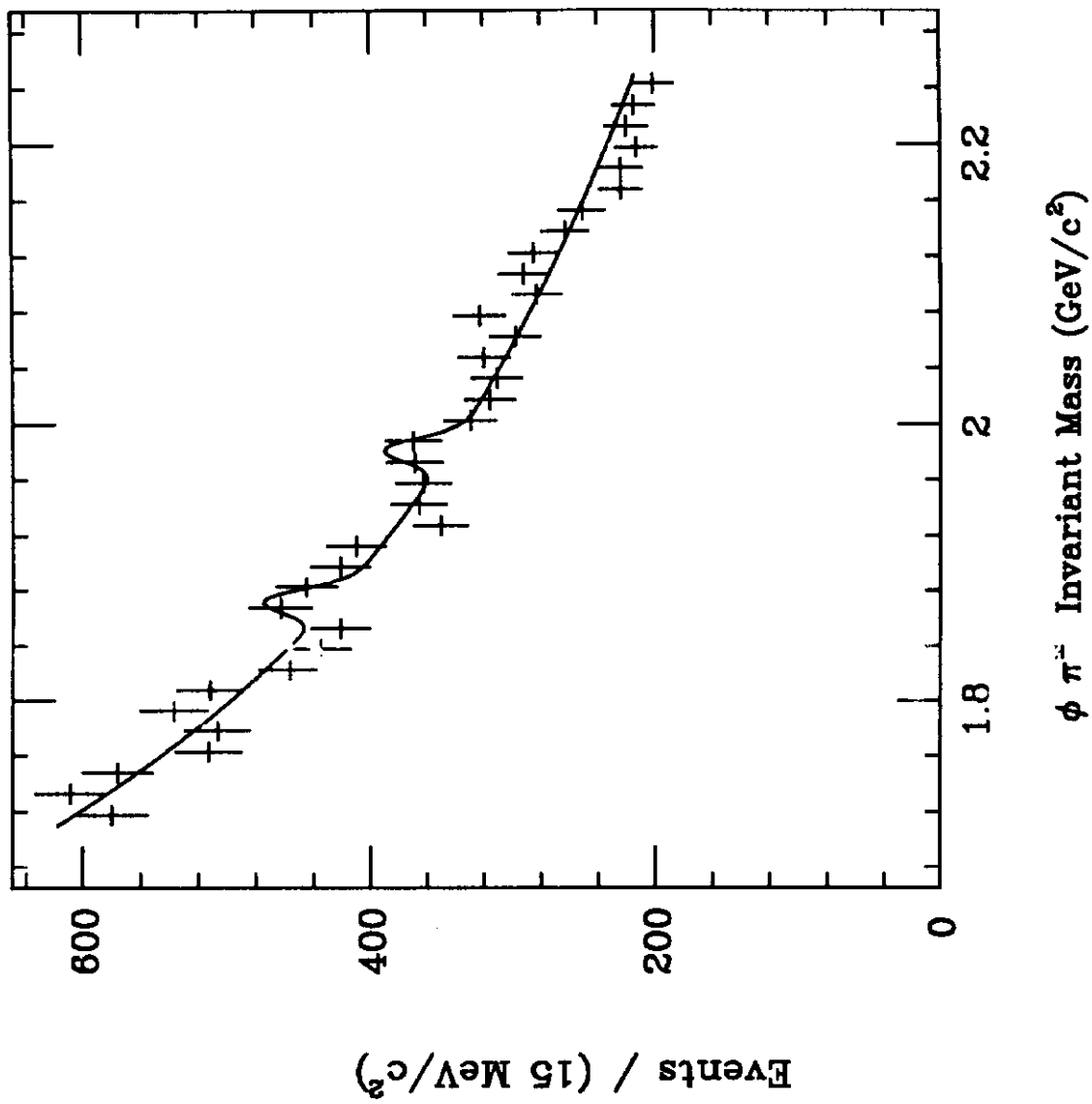


Fig. 2

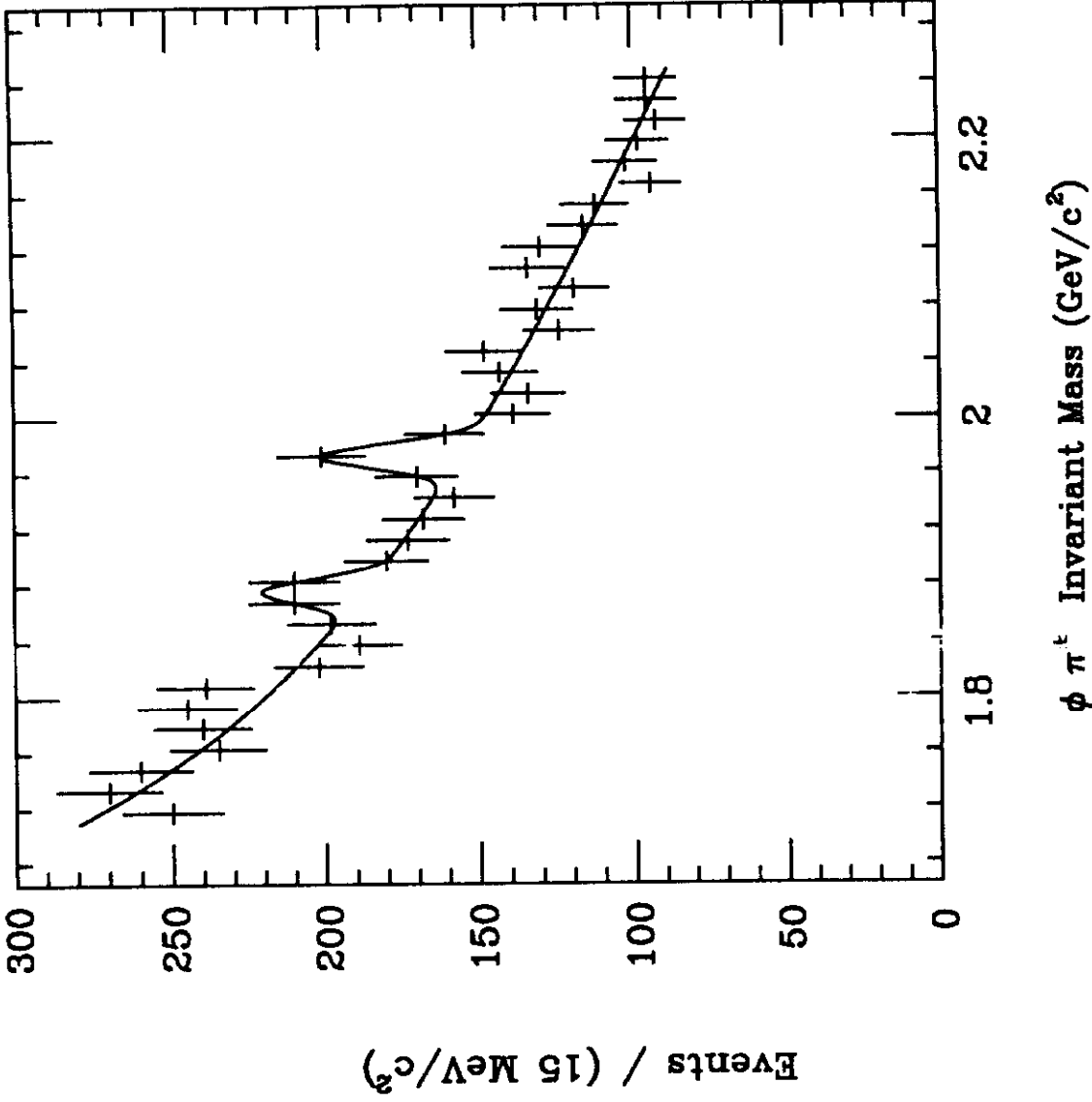


Fig. 3